Up-converted emission in Pr^{3+}-doped fluoride nanocrystals-based oxyfluoride glass ceramics

Hairong Zheng[a], Xiao-jun Wang[b,c,*], M.J. Dejneka[d], W.M. Yen[a], R.S. Meltzer[a]

[a] Department of Physics and Astronomy, University of Georgia, Athens, GA 30602, USA
[b] Key Laboratory of Excited State Processes, Changchun Institute of Optics, Fine Mechanics, and Physics, Chinese Academy of Sciences, Changchun 130033, China
[c] Department of Physics, Georgia Southern University, Statesboro, GA 30460, USA
[d] Corning, Inc., Corning, NY 14831 USA

Abstract

Red-to-blue up-converted emission has been studied for Pr^{3+}-doped fluoride nanocrystals-based oxyfluoride glass ceramics. Emission by the $^3P_0$–$^3H_4$ transition has been observed upon excitation of the $^1D_2$ manifold. The concentration, wavelength and flux dependence of the up-conversion have been investigated at different temperatures from 1.5 K at high spectral resolution. Excitation spectra indicate that the most efficient excitation is at 591.6 nm, which corresponds to the transition of $^1D_2$ (II), the second-lowest level of the $^1D_2$ manifold. The intensity of the blue emission shows a quadratic dependence on the incident flux. The dynamical processes of this up-conversion have also been examined, suggesting that the energy-transfer process is responsible for the up-converted emission. The different spectroscopic features between nanocrystals and bulk crystals have been characterized, indicating that the local temperature in the nanocrystals is higher than that in bulk crystals due to the lower thermal conductivity of the glass matrix.
© 2004 Elsevier B.V. All rights reserved.

Keywords: Nano-crystals; Up-conversion; LaF_3:Pr^{3+}

1. Introduction

Up-converted emission in rare-earth (RE)-doped systems has been widely studied because of its broad applications for laser materials and fibre optics. Among the RE ions, trivalent praseodymium (Pr^{3+}) is an attractive optical activator since there exist several metastable states in its energy-level spectrum, such as the $^1G_4$, $^1D_2$, and $^3P_0$ manifolds, which may exhibit stimulated emission from the infra-red to blue. The states with the lower decay rate, such as $^1D_2$, also enhance the possibility of sequential two-photon absorption using these states as intermediate levels. Anti-Stokes blue emission from the $^3P_0$ state has been observed upon excitation of the $^1D_2$ manifold of both bulk crystals [1–4] and glass hosts [5–8]. Two dominant up-conversion mechanisms have been discussed for these systems: (1) cooperative energy transfer involving a pair of Pr^{3+} ions, which has been observed in LaF_3:Pr^{3+}

[1,2], KPb_2Cl_5:Pr^{3+} [6], and some Pr^{3+}-doped glasses [5,7,8]; and (2) sequential two-photon absorption or excited-state absorption involving a single Pr^{3+} centre, which has also been observed for a crystal host ($La_2Ti_2O_7$:Pr^{3+}) [9] and glass hosts [4,10].

Oxyfluoride glass ceramics are newly developed materials in the past 10 years, which offer low phonon energies enabling emission from the RE energy levels that may be quenched in high-phonon energy glasses [11]. Pr^{3+}-doped oxyfluoride glasses are of great interest for their optical and fluorescence properties and have potential use in fibre amplifiers, up-conversion lasers, and displays. When the ceramics are annealed, LaF_3 nanocrystals containing active RE ions form with optical properties nearly identical to those of bulk-sample crystals. The RE solubility and thermal and environmental stability have been greatly improved [12] for fluoride nanocrystals-based oxyfluoride glass ceramics since they were first reported in 1993 [13].

In this paper, red-to-blue up-converted emission involving the $^1D_2$ manifolds is reported for Pr^{3+}-doped fluoride nanocrystals-based oxyfluoride glass ceramics at different temperatures from 1.5 K. The optical emission and excitation spectra were investigated. The excitation spectra indicate that the most efficient excitation is at 591.6 nm, which corresponds to the $^3H_4$ (I) → $^1D_2$ (II) transition. The intensity of the blue emission shows a quadratic dependence on the incident flux. The dynamical processes of this up-conversion have also been examined, indicating that the energy-transfer process dominates the observed up-converted emission. Differences in the spectroscopic properties between the nanocrystals and bulk crystals are characterized, and they indicate that the local temperature in nanocrystals is higher than that in the bulk crystal due either to the lower thermal conductivity of glass matrix or to confinement within the nanocrystal.

2. Experimental

Transparent oxyfluoride glass samples were prepared by Corning, Inc., by melting the appro-priate batch materials [12]. Pr-doped nanocrystals are formed within the glass with sizes of ~ 20 nm, and these sizes could be controlled by the heat-treatment temperature. While the average concentration of Pr^{3+} in a given sample ranges from 0.1% to 0.5%, during the heat-treatment process, the Pr^{3+} ions partition into LaF_3 crystals, causing the concentration of Pr^{3+} in the nanocrystals to be several times higher than the average value of the glass ceramic. The fluorescence measurements were made with a 0.75 m SPEX 1702 spectrometer equipped with a cooled PMT. A Spectra Physics/ Quanta Ray Nd:YAG (DCR-1) pumped PDL dye laser was used as a pulsed-excitation source. The fluorescence decay was recorded using a Tektronix TDS 460A digital oscilloscope. Low temperature measurements were made with either a liquid helium cryostat or an RMC Helium Closed-Cycle Cryosystem.

3. Results and discussion

Fig. 1 shows the absorption spectrum around the $^1D_2$ manifold of Pr^{3+}-doped nanocrystals at 1.5 K (dashed line) and 15 K (solid line). The strongest absorption occurs for the transition to the $^1D_2$ (II) level, the second-lowest energy level of the $^1D_2$ manifold at a wavelength of 591.6 nm. Transitions from higher-lying levels of the $^3H_4$ manifold were observed at 15 K. Fig. 2 shows the

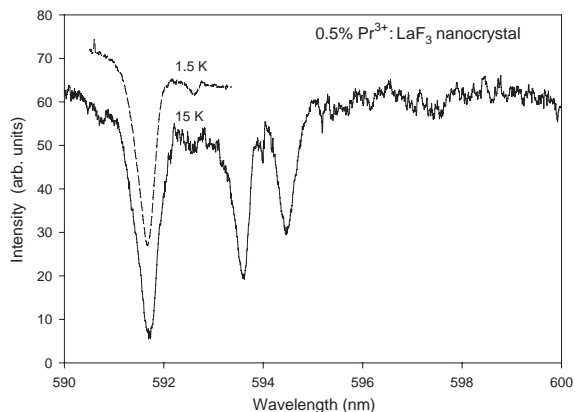Fig 1. Absorption spectra for the $^1D_2$ manifold region of Pr^{3+}-doped nanocrystals at 1.5 and 15 K.

up-converted emission spectra for both a Pr^{3+}-doped bulk crystal (Fig. 2(b)) and Pr^{3+}-doped nanocrystals (Fig. 2(a)) with pulsed-laser excitation of the absorption transition at 591.6 nm to the $^1D_2$ (II) level at 15 K. The average concentration of Pr^{3+} in the ceramic is 0.1%, yielding a concentration inside the nanocrystals close to that in the bulk crystal (0.5%) [14]. Peak A, at 477.8 nm, is the zero-phonon line emission ($^3P_0 \rightarrow {}^3H_4$ (I)). Peaks B, C, D, E, and F correspond, respectively, to the $^3P_0 \rightarrow {}^3H_4$ (II, 57 cm^{-1}), $^3P_0 \rightarrow {}^3H_4$ (III, 73 cm^{-1}), $^3P_0 \rightarrow {}^3H_4$ (IV, 136 cm^{-1}), $^3P_0 \rightarrow {}^3H_4$ (V, 196 cm^{-1}), and $^3P_0 \rightarrow {}^3H_4$ (VI, 204 cm^{-1}) [15] transitions from the $^3P_0$ level to excited states of the $^3H_4$ manifold.

Fig. 3 depicts the excitation spectra for the Pr^{3+}-doped bulk crystal (Fig. 3(b)) and Pr^{3+}-doped nanocrystals (Fig. 3(a)) when monitoring the emission at 479.1 nm. It is interesting to notice the differences between the two spectra measured at the same nominal temperature of 15 K: in addition to the broadened feature in the spectral range of 591.0–592.0 nm, two excitation peaks, at 593.5 and 594.4 nm, are observed in the nanocrystals but only very weakly in the bulk crystals (see the inset in the figure). These two peaks are due to
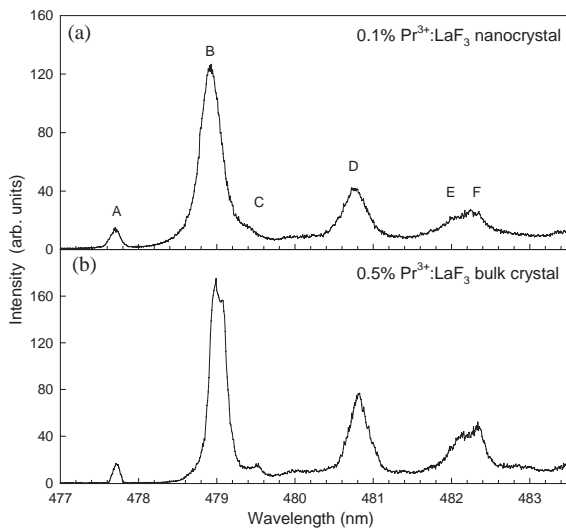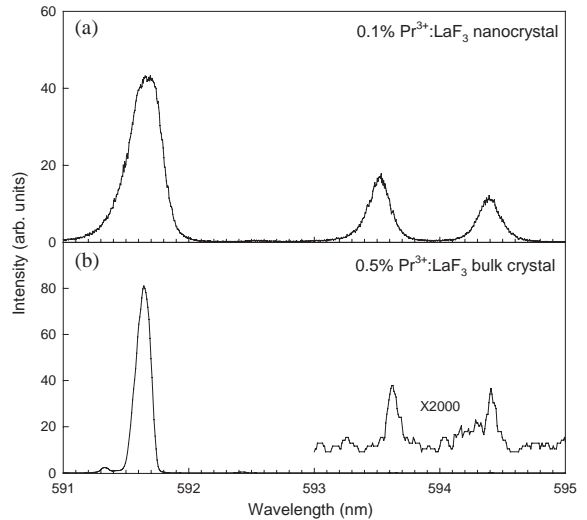

Fig 3. Excitation spectra for Pr^{3+}-doped nanocrystals (Fig. 3(a)) and a Pr^{3+}-doped bulk crystal (Fig. 3(b)) when monitoring the emission at 479.1 nm, at 15 K.

Fig 2. Up-converted emission spectra for both Pr^{3+}-doped nanocrystals (Fig. 2(a)) and a Pr^{3+}-doped bulk crystal (Fig. 2(b)) with pulsed-laser excitation of the $^1D_2$ (II) level at 591.6 nm, at 15 K.

the transitions $^3H_4$ (II, 57 cm^{-1}) $\rightarrow {}^1D_2$ and $^3H_4$ (III, 73 cm^{-1}) $\rightarrow {}^1D_2$, suggesting that the electron populations of these states, and therefore the local temperature, are higher in the nanocrystals than in the bulk crystal. This may be understood by considering the fact that the nanocrystals are embedded in the glass matrix which has a much lower thermal conductivity than the crystal. When the dye laser is tuned to the resonant transitions of Pr^{3+} in nanocrystals, a much larger fraction of the excitation energy is absorbed by these Pr^{3+} ions in the nanocrystals than in the glass host. The heat generated by one laser pulse may not be released from the region of the nanocrystals between the pulses so that the system may not be in thermal equilibrium. The intensity ratio of $^3H_4$ (II, 57 cm^{-1}) $\rightarrow {}^1D_2$ to $^3H_4$ (I) $\rightarrow {}^1D_2$ can be estimated from Fig. 3(a) with a value of ~ 0.4. This ratio should be proportional to the square of the oscillator-strength ratio of the same transitions and to the square of the occupation-number ratio of the $^3H_4$ (II, 57 cm^{-1}) to $^3H_4$ (I), since the excitation spectra are obtained from up-converted emission, which occurs by an energy-transfer cross relaxation process involving a pair of excited ions (as described in the next paragraph). The oscillator-strength ratio can be estimated from Fig. 3(b)

assuming that the crystal, with high thermal conductivity, is in thermal equilibrium with the bath, i.e., (oscillator-strength ratio)^2(occupation-number ratio)^2 = 2/17,000. At 15 K, the oscillator-strength ratio is found to have a value of 2.5. The local temperature in the nanocrystals is then estimated using this ratio and the same product of squares of ratios to be 29 K compared to the nominal bath temperature of 15 K.

Fig. 4 represents the decay curves of the up-converted emission with two different concentrations. A rise time is observed for both samples which rules out the possibilities of either two-photon absorption (there is no appropriate energy levels for the direct two-photon absorption) or sequential two-photon excitation processes. Energy transfer involving a pair of Pr^{3+} ions is believed to be responsible for the observed up-conversion [1–2]. The concentration dependence of the temporal behaviour supports the energy-transfer mechanism, as shown in Fig. 4. The respective rise and decay times change from 16 and 90 μs for 0.1% Pr^{3+} to 1.6 μs and 41 μs for 0.5% Pr^{3+}. The short rise time of 1.6 μs suggests that the mechanism of excitation annihilation involving pairs of ions in the $^3H_6$ and $^1D_2$ states does not account for the energy-transfer process. The reason is that the population build-up of $^3H_6$ due to the multi-phonon relaxation from the $^1D_2$ state requires a much longer time than 1.6 μs (it should be on the order of the decay time of $^1D_2$). Phonon-

assisted energy transfer between two ions excited to the $^1D_2$ state [2,16] must thus dominate the up-conversion, which could result in a very short rise time, but a slow decay. In this process, a cross-relaxation energy transfer occurs whereby one Pr^{3+} ion in the $^1D_2$ state undergoes a transition to $^1G_4$ and another ion in $^1D_2$ makes a transition to $^3P_2$ with the assistance of phonon emission. The linear and quadratic dependence on excitation intensity of the observed $^1D_2$ emission and up-converted $^3P_0$ emission, respectively, also supports this energy-transfer mechanism.

In summary, we have observed the red-to-blue up-converted emission of Pr^{3+}-doped LaF_3 upon excitation of the $^1D_2$ manifold. Different spectroscopic features between the nanocrystals and bulk crystals have been characterized, indicating that the local temperature in nanocrystals is higher than that in the bulk crystal, most likely from the lower thermal conductivity of the glass matrix. The intensity of the blue emission shows a quadratic dependence on the incident flux. The dynamical processes of the up-conversion have also been examined, indicating the energy-transfer process as the origin of the observed up-converted emission.

Acknowledgements

Fig 4. Decay curves of the up-converted emission for two different Pr^{3+} concentrations (0.1% and 0.5%) at 1.5 K.

References

[1] D.J. Zalucha, J.C. Wright, F.K. Fong, J. Chem. Phys. 59 (1973) 997.

[2] J.C. Vial, R. Buisson, F. Madeore, M. Poirier, J. Phys. (Paris) 40 (1979) 913.

[3] A. Lezama, M. Oria, J.R.R. Leite, C.B. Dearaujo, Phys. Rev. B 32 (1985) 7139.

[4] E.M. Pacheco, C.B. De Araujo, Chem. Phys. Lett. 148 (1988) 334.

[5] J. Fernandez, R. Balda, A. Mendioroz, A.J. Garcia-Adeva, J. Phys. Condens. Mater. 13 (2001) 10347.

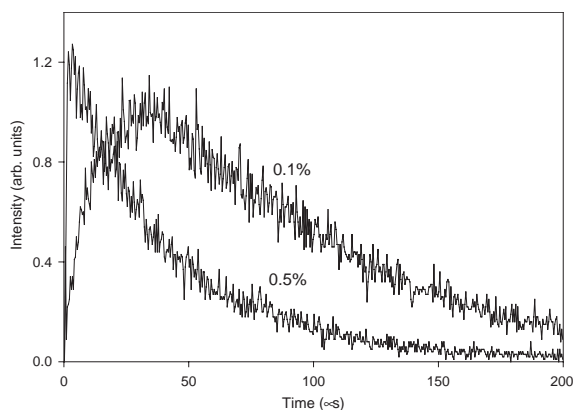[6] R. Balda, M. Voda, M. Al-Saleh, J. Fernandez, J. Lumin. 97 (2002) 190.

[7] L.E.E. De Araujo, A.S.L. Gomes, C.B. De Araujo, Y. Messaddeq, A. Florez, M.A. Aegerter, Phys. Rev. B 50 (1994) 16219.

[8] R. Balda, J. Fernandez, A. de Pablos, J.M. Fdez-Navarro, J. Phys. Condens. Mater. 11 (1999) 7411.

[9] P.T. Diallo, P. Boutinaud, R. Mahiou, J. Alloys Compounds 323 (2002) 139.

[10] R. Balda, I.S. de Ocariz, J. Fernandez, J.M. Fdez-Navarro, M.A. Arriandiaga, J. Phys. Condens. Mater. 12 (2000) 10623.

[11] M.J. Dejneka, MRS Bull. 23 (1998) 57.

[12] M.J. Dejneka, J. Non-Crysat. Solids 239 (1998) 149.

[13] Y. Wang, J. Ohwaki, Appl. Phys. Lett. 63 (1993) 3268.

[14] X.J. Wang, S.H. Huang, R. Reeves, W. Wells, M.J. Dejneka, R.S. Meltzer, W.M. Yen, J. Lumin. 94/95 (2001) 229.

[15] W.M. Yen, W.C. Scott, A.L. Schawlow, Phys. Rev. 136 (1A) (1964) A271.

[16] F. Auzel, Proc. IEEE 61 (1973) 758.